

Light curves of oscillating neutron stars

Umin Lee^{1★} and Tod E. Strohmayer^{2★}

¹*Astronomical Institute, Tohoku University, Sendai, Miyagi 980-8578, Japan*

²*Laboratory for High Energy Astrophysics, NASA Goddard Space Flight Center, Greenbelt, MD 20771, USA*

Accepted 2005 May 12. Received 2005 April 9; in original form 2005 February 23

ABSTRACT

We calculate light curves produced by r modes with small azimuthal wavenumbers, m , propagating in the surface fluid ocean of rotating neutron stars. We include relativistic effects due to rapid rotation, and propagate photons from the stellar surface to a distant observer using the Schwarzschild metric. The wave motions of the surface r modes are confined to the equatorial region of the star, and the surface pattern of the temperature variation can be either symmetric (for even modes) or antisymmetric (for odd modes) with respect to the equator. Because for the surface r modes the oscillation frequency in the corotating frame of the star is much smaller than the rotation frequency, Ω , we employ the approximation in which the oscillation frequency in the inertial frame, σ , is given by $\sigma = -m\Omega$. We find that the even, $m = 1$ r mode produces the largest light variations. The dominant Fourier component in the light curves of these modes is the fundamental having $\sigma = -\Omega$, and the first harmonic component having $\sigma = -2\Omega$ is always negligible in comparison. The dominant Fourier component of the even, $m = 2$ r modes is the first harmonic. Although the odd r modes produce smaller amplitude light variations compared with the even modes, the light curves of the former have a stronger first harmonic component. If both $m = 1$ and 2 r modes are excited simultaneously, a rich variety of light curves is possible, including those having an appreciable first harmonic component. We show that the phase difference, $\delta - \delta_E$, between the bolometric light curve and that at a particular photon energy can possibly be used as a probe of the stellar compactness, R/M , where R and M are the radius and mass of the star. We find that hard leads are expected in general rather than hard lags, although there exists a parameter space of R and the inclination angle i that produces hard lags for the odd modes.

Key words: stars: neutron – stars: oscillations – stars: rotation.

1 INTRODUCTION

It is now widely accepted that millisecond oscillations during thermonuclear X-ray bursts (hereafter, burst oscillations) on accreting, weakly magnetized neutron stars in low-mass X-ray binary (LMXB) systems are produced by spin modulation of a slowly moving, non-uniform brightness pattern on the stellar surface (see Strohmayer et al. 1996; Strohmayer & Bildsten 2004; van der Kils 2004). In addition to revealing the spin frequency, these oscillations encode information about the global properties of the neutron star. A number of attempts have been made to model burst oscillations and thus to infer these properties (e.g. Muno, Özel & Chakrabarty 2002b; Nath, Strohmayer & Swank 2002; Poutanen & Gierliński 2003; Bhattacharyya et al. 2005); however, uncertainties associated with the exact nature of the brightness pattern make a unique interpretation of the data problematic.

As of 2005 February, the number of LMXBs that exhibit burst oscillations amounts to 14, and two of these contain millisecond X-ray pulsars (see, for example, Chakrabarty et al. 2003; Strohmayer et al. 2003). For most burst oscillations a single oscillation frequency is found that displays a positive frequency drift $\Delta\nu_{\text{burst}}$ of a few Hz from the start to the tail of a burst. In the decaying tail, the frequency often approaches an asymptotic value (e.g. Strohmayer & Markwardt 1999). The asymptotic frequencies are stable to a few parts in 1000 in bursts observed over several years from any given source (Strohmayer et al. 1998b; Muno, Chakrabarty & Galloway 2002a). Background subtracted light curves for the burst oscillations are in most cases well fitted by a single sinusoid, the frequency of which we will call the fundamental frequency. Harmonic content in the light curves is generally small (Strohmayer & Markwardt 1999; Muno, Özel & Chakrabarty 2002b). Indeed, to date there exists only one strong detection of a first harmonic, in the millisecond X-ray pulsar XTE J1814–338 (Strohmayer et al. 2003; Bhattacharyya et al. 2005). On average, the rms amplitudes of the burst oscillations are 2–10 per cent, and generally increase with photon energy (Muno,

★E-mail: lee@astr.tohoku.ac.jp (UL); stroh@clarence.gsfc.nasa.gov (TES)

Özel & Chakrabarty 2003). Muno et al. (2003) also explored the energy dependence of the oscillation phases of burst oscillations. They found either constant phase lags with energy or in some cases evidence for modest hard lags, behaviour that is opposite to what one would expect from relativistic motion of a simple hotspot on the stellar surface (e.g. Ford 1999). Interestingly, where phase lags have been measured in the accreting millisecond pulsars they all show soft lags, consistent with a rotating hotspot model (Cui, Morgan & Titarchuk 1998; Poutanen & Gierliński 2003).

As noted above, a non-uniform brightness distribution on the surface of rotating neutron stars is almost certainly responsible for the burst oscillations, and several models have so far been proposed to explain the inhomogeneous pattern. As a typical model, Strohmayer et al. (1997) suggested the oscillation originates from hot regions (hotspots) in a thermonuclear burning layer that expands and decouples from the neutron star at the start of the burst. Although a simple hotspot appears to be consistent with oscillations observed during the onset of some bursts (see Strohmayer et al. 1998a), further calculations have suggested that a rigidly rotating, hydrostatically expanding burning layer produces too small a frequency drift (Cumming & Bildsten 2000; Cumming et al. 2002).

There have been numerous efforts to calculate light curves produced by hotspots on the surface of rotating neutron stars (e.g. Pechenick, Ftacis & Cohen 1983; Chen & Shaham 1989; Strohmayer 1992; Page 1995; Braje, Romani & Rauch 2000; Weinberg, Miller & Lamb 2001; Muno et al. 2002b; Nath, Strohmayer & Swank 2002; Poutanen & Gierliński 2003; Bhattacharyya et al. 2005). In the modelling of the light curves, many parameters are employed, for example, the number of hotspots, their location with respect to the rotation axis, their angular sizes, the inclination angle between the line of sight and the rotation axis, the angular dependence of the specific intensity, the temperature of the spots, the temperature contrast between the spots and their surroundings, the mass, radius, and spin frequency of the star. As noted above, burst oscillation light curves are remarkably sinusoidal. Although the light-curve amplitudes are dependent on the relativistic parameter R/M , which is a parameter of particular importance, it is obvious that there remain parameters other than R/M that affect the amplitudes, such as the angular sizes and locations of the hotspots and the inclination angle (e.g. Pechenick et al. 1983; Weinberg et al. 2001; Muno et al. 2002b). In this sense it is quite important to find other observational quantities that can be used to obtain independent constraints on these parameters. The energy dependences of phase lags are an example of potentially important observational quantities that carry useful information about the neutron star. Taking account of the special relativistic Doppler boosting of X-ray photons due to rapid rotation of the star (Ford 1999; Weinberg et al. 2001), the hotspot model can produce hard lags more or less consistent with those observed in the millisecond X-ray pulsar SAX J1808.4–3658 and IGR J00291+5934 (Poutanen & Gierliński 2003; Galloway et al. 2005), but the model appears to be at odds with the suggestion of hard lags in some burst oscillations (Muno et al. 2003). Although it may be possible to produce hard lags via a hot Comptonizing corona, it is worth exploring in more detail whether more complex brightness patterns (such as oscillation mode patterns) on the stellar surface might be consistent with the production of hard lags.

By inferring the hotspot size using the observationally obtained blackbody flux F_{bb} , Poutanen & Gierliński (2003) have succeeded in estimating the radius of the millisecond X-ray pulsar SAX J1808.4–3658 assuming an appropriate range of mass for the star.

Recently, Strohmayer et al. (2003) have found the first harmonic component in the light curves of burst oscillations from the accreting millisecond X-ray pulsar XTE J1814–338, and Bhattacharyya et al. (2005) obtained a useful constraint on the ratio R/M assuming a single hotspot model.

As alluded to above, the hotspot model is not always successful in producing the observed light curves of the burst oscillations. As discussed by Muno et al. (2002b), a small hotspot in a completely dark background is likely to produce light curves with too large an amplitude as well as having strong harmonic components not seen observationally. To suppress the large amplitudes and the harmonics, we have to assume, for example, a hotspot of angular size $\alpha \sim \pi/2$ or almost completely antipodal hotspots, the assumptions of which are not necessarily physically well motivated. It is therefore important to pursue alternatives to the hotspot model.

In this paper, we calculate light curves of rotating neutron stars assuming the surface temperature perturbation pattern caused by surface r modes propagating in the fluid ocean of a mass accreting neutron star (Lee 2004). It was Heyl (2004) who first argued that the r modes with low m may play a possible role for burst oscillations. The surface r modes are rotationally induced oscillations with very low frequencies in the corotating frame of the star. The r modes have dominant vorticity $(\nabla \times \mathbf{v})_r$, and are basically just large-scale vortices (see Spitkovsky, Levin & Ushomirsky 2002). If we assume axisymmetry of the equilibrium configuration of the rotating star, the time dependence of the temperature perturbation may be given by $e^{i\sigma t}$, where σ denotes the oscillation frequency in the inertial frame. If we let ω and Ω denote the oscillation frequency in the corotating frame and the spin frequency of the star, respectively, we have $\sigma = \omega - m\Omega$, which leads to $\sigma \approx -m\Omega$ for the surface r modes, because $|\omega| \ll |m\Omega|$, where m is an integer representing the azimuthal wavenumber around the rotation axis. The time dependence of the perturbation is thus to good approximation given by $e^{-im\Omega t}$. Because only the oscillation modes having low m will produce light variations of appreciable amplitude, in this paper, we only consider the surface r modes with $m = 1$ or $m = 2$. We briefly describe the method of calculation in Section 2. In Section 3 we discuss some of our numerical results with relevance to burst oscillations. In Section 4 we give a discussion, and we give a summary of our principal conclusions in Section 5.

2 METHOD OF SOLUTION

The method of calculating light curves of rotating neutron stars is similar to those discussed by Pechenick et al. (1983), Page (1995) and Weinberg et al. (2001). Instead of presuming the presence of a hotspot on the surface of a rotating neutron star, we assume that the temperature varies across the surface with the angular distribution appropriate for a surface r mode propagating in the fluid ocean of the star. The surface r modes, which have very low oscillation frequencies in the corotating frame of the star, can plausibly be excited during thermonuclear bursts (Lee 2004).

To describe oscillations of rotating neutron stars, we employ an xyz coordinate system whose origin is at the centre of the star with the rotation axis along the z -direction. For convenience, we also assume that the observer is in the x - z plane. In this coordinate system, the oscillations of rotating neutron stars are described by employing spherical polar coordinates (r, θ, ϕ) with the axis $\theta = 0$ being the z -axis. Then, the displacement vector $\xi(r, \theta, \phi, t)$ is

given by

$$\xi_r = \sum_{j=1}^{\infty} S_{lj} Y_{lj}^m e^{i\sigma t}, \quad (1)$$

$$\xi_\theta = \sum_{j=1}^{\infty} \left(H_{lj} \frac{\partial}{\partial \theta} Y_{lj}^m + T_{lj} \frac{1}{\sin \theta} \frac{\partial}{\partial \phi} Y_{lj}^m \right) e^{i\sigma t}, \quad (2)$$

$$\xi_\phi = \sum_{j=1}^{\infty} \left(H_{lj} \frac{1}{\sin \theta} \frac{\partial}{\partial \phi} Y_{lj}^m - T_{lj} \frac{\partial}{\partial \theta} Y_{lj}^m \right) e^{i\sigma t}, \quad (3)$$

and the Lagrangian perturbation of the temperature is given by

$$\delta T = \sum_{j=1}^{\infty} \delta T_{lj} Y_{lj}^m e^{i\sigma t}. \quad (4)$$

Here, σ is the oscillation frequency in the inertial frame, and Y_l^m denotes the spherical harmonic function with degree l and azimuthal wavenumber m , and $l_j = |m| + 2(j-1)$ and $l'_j = l_j + 1$ for even modes, and $l_j = |m| + 2(j-1) + 1$ and $l'_j = l_j - 1$ for odd modes, and $j = 1, 2, \dots$. The functions $\xi(r, \theta, \phi, t)$ and δT are obtained as a solution to linear differential equations for oscillations of a rotating star, and we need to specify a normalization condition to determine the amplitudes. Because the surface r modes have dominant toroidal components T_{lj} , we will employ the amplitude normalization given by $|\text{Re}[i T_{lj}(R)/R]| = 1$.

The surface temperature of a rotating star that pulsates in various oscillation modes may formally be given by

$$T(R, \theta, \phi, t) = T_0 + \text{Re} \left\{ \sum_{\alpha} C_{\alpha} \left[\sum_{j \geq 1} \delta T_{lj}^{\alpha}(R) Y_{lj}^m(\theta, 0) \right] \times e^{i(m\phi + \sigma_{\alpha} t)} \right\}, \quad (5)$$

where T_0 is the mean surface temperature, α indicates a combination of indices that distinguish various oscillation modes, and σ_{α} and C_{α} denote, respectively, the oscillation frequency and a complex constant representing the amplitudes of the oscillation mode α . Note that by introducing C_{α} in equation (5) we mean $|\text{Re}[i T_{lj}^{\alpha}(R)/R]| = |C_{\alpha}|$. Using the oscillation frequency $\omega = \sigma + m\Omega$ in the corotating frame, we have

$$m\phi + \sigma_{\alpha} t = m\hat{\phi} + \omega_{\alpha} t, \quad (6)$$

where $\hat{\phi} = \phi - \Omega t$ is the longitude in the corotating frame.

To consider photon trajectories around a neutron star, it is convenient to introduce another coordinate system $x'y'z'$, for which the origin is at the centre of the star, and the z' -axis is pointing to the observer and $y = y'$. If we let i denote the inclination angle between the z -axis and the z' -axis, we have

$$\begin{aligned} x &= x' \cos i + z' \sin i, & y &= y', \\ z &= -x' \sin i + z' \cos i, \end{aligned} \quad (7)$$

and it is easy to derive the relation between the two spherical polar coordinate systems (r, θ, ϕ) and (r', θ', ϕ') , where the axis of $\theta' = 0$ is the z' -axis.

If we assume the Schwarzschild metric around the neutron star with mass M and radius R , the number flux, per photon energy E_{∞} , of thermal photons emitted from the stellar surface and received by

a distant observer may be given by (e.g. Page 1995)

$$\begin{aligned} \frac{1}{S} \frac{d^2 N(E_{\infty})}{dt_{\infty} dE_{\infty}} &= \frac{2\pi}{c^2 h^3} \frac{R_{\infty}^2}{D^2} E_{\infty}^2 \int_0^1 2q dq \int_0^{2\pi} \\ &\times \frac{d\phi'}{2\pi} \frac{1}{e^{f e^{-\eta} E_{\infty}/k_B T} - 1} \\ &\equiv \frac{2\pi}{c^2 h^3} \frac{R_{\infty}^2}{D^2} \frac{E_{\infty}^2}{e^{E_{\infty}/k_B T_0} - 1} G_{E_{\infty}}(t_{\infty}), \end{aligned} \quad (8)$$

and integrating equation (8) with respect to the variable E_{∞} leads to

$$\begin{aligned} \frac{1}{S} \frac{dN(E_{\infty})}{dt_{\infty}} &= 2.404 \times \frac{2\pi}{c^2 h^3} \frac{R_{\infty}^2}{D^2} \int_0^1 2q dq \int_0^{2\pi} \frac{d\phi'}{2\pi} \left(\frac{k_B T}{f e^{-\eta}} \right)^3 \\ &\equiv \frac{4.808\pi}{c^2 h^3} \frac{R_{\infty}^2}{D^2} \left(\frac{k_B T_0}{e^{-\eta}} \right)^3 G(t_{\infty}). \end{aligned} \quad (9)$$

Here, D is the distance to the observer, T is the surface temperature, k_B is the Boltzmann constant, c is the velocity of light, and h is the Planck constant. We have neglected, for simplicity, the interstellar absorption effect and the dependence of the effective area S of the detector on the photon energy. Here,

$$R_{\infty} = e^{-\eta} R \quad (10)$$

is the radius of the star seen by a distant observer, and $dt_{\infty} = e^{-\eta} dt$ denotes the increment of the coordinate time t_{∞} , where

$$e^{\eta} = \sqrt{1 - R_G/R}, \quad (11)$$

$R_G = 2GM/c^2$ is the Schwarzschild radius, and dt is the increment of the proper time at the surface of the star. Note that $\Omega_{\infty} = e^{\eta} \Omega$ because $\Omega_{\infty} dt_{\infty} = \Omega dt$, where Ω_{∞} is the angular spin frequency of the star seen from infinity. If we let E_e and E_{∞} denote, respectively, the photon energy in the corotating frame of the star at the surface and the photon energy received by a distant observer, we have

$$E_e = f e^{-\eta} E_{\infty}, \quad (12)$$

where the factor f , representing the Doppler shift in the photon energy from $e^{-\eta} E_{\infty}$ in the non-rotating frame at the stellar surface to E_e in the corotating frame, is given by

$$f = \gamma (1 - \mathbf{v} \cdot \mathbf{o}/c). \quad (13)$$

Here, $\mathbf{v} = \Omega \times \mathbf{R} = R\Omega \sin \theta \mathbf{e}_{\phi}$ where \mathbf{e}_{ϕ} is the unit vector in the azimuthal direction, \mathbf{o} is the unit vector along the trajectory of a photon at the surface, and $\gamma = 1/\sqrt{1 - v^2/c^2}$. Note that the four vector of a photon in the non-rotating frame may be given by $o^{\mu} = e^{-\eta} E_{\infty}(1, \mathbf{o})$. Using the angle $\zeta(\theta')$ between the local normal and the photon trajectory, at the surface, reaching the observer at infinity, the variable q in equations (8) and (9) is defined by

$$q \equiv \sin \zeta, \quad (14)$$

and the relation between θ' and q is determined by the integration given by

$$\theta'(q) = \int_0^{R_G/2R} \frac{q du}{\sqrt{(1 - R_G/R) R_G/2R - (1 - 2u)u^2 q^2}}. \quad (15)$$

The maximum value θ'_{\max} occurs when $q = 1$ and is shown as a function of the radius R in Fig. 1 for $M = 1.4 M_{\odot}$ (solid line) and for $M = 2 M_{\odot}$ (dashed line). Because \mathbf{o} at the stellar surface is given by

$$\mathbf{o} = \sin(\theta' - \zeta) \cos \phi' \mathbf{i}' + \sin(\theta' - \zeta) \sin \phi' \mathbf{j}' + \cos(\theta' - \zeta) \mathbf{k}', \quad (16)$$

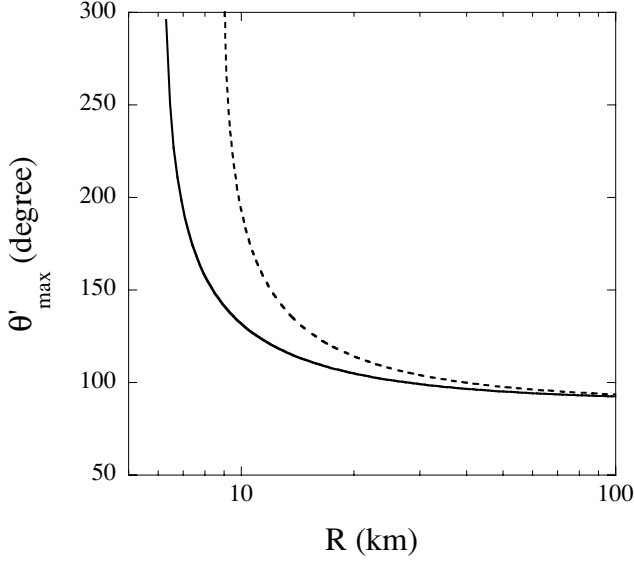


Figure 1. θ'_{\max} as a function of the radius R for $M = 1.4 M_{\odot}$ (solid line) and $M = 2 M_{\odot}$ (dashed line).

where \mathbf{i}' , \mathbf{j}' and \mathbf{k}' are the orthonormal vectors parallel to the x' -, y' - and z' -axes, respectively, we have

$$\frac{\mathbf{v} \cdot \mathbf{o}}{\Omega R \sin \theta} = \sin(\theta' - \zeta) (\cos \phi \sin \phi' - \sin \phi \cos \phi' \cos i) - \cos(\theta' - \zeta) \sin \phi \sin i. \quad (17)$$

Note that without light bending so that $\theta' = \zeta$, we simply have $\mathbf{v} \cdot \mathbf{o} = -\Omega R \sin \phi \sin i \sin \theta$. The aberration effect may be given by

$$\cos \zeta_e = \frac{e^{-\eta} E_{\infty}}{E_e} \cos \zeta, \quad (18)$$

where ζ_e is the angle measured in the corotating frame of the star.

For waves whose ϕ and t dependence is given by $e^{im\phi + i\sigma t}$, it is easy to incorporate the time-delay effect that arises because of the difference in the path lengths of photons emitted from different points on the surface of the star. Because the traveltime of a photon from a point having the impact parameter $b = qR_{\infty}$ at the surface of the star to an observer at infinity is given by

$$t_{\infty}(b) = \frac{R_G}{c} \int_R^{\infty} \frac{1}{\sqrt{1 - (1 - R_G/r)(b/r)^2}} \left(1 - \frac{R_G}{r}\right)^{-1} \frac{dr}{R_G}, \quad (19)$$

the time lag may be defined by

$$\Delta t_{\infty}(b) \equiv t_{\infty}(b) - t_{\infty}(0). \quad (20)$$

Replacing t_{∞} by $t_{\infty} - \Delta t_{\infty}(b)$, we rewrite the time and ϕ dependence $e^{im\phi + i\sigma t}$ of the perturbations as

$$e^{im\phi + i\sigma t} e^{-ie^{\eta} \sigma \Delta t_{\infty}(b)} \quad (21)$$

so that we can take account of the time-lag effects in light-curve calculations (see, for example, Cadeau, Leahy & Morsink 2005).

For the light curves $G(t)$ or $G_{E_{\infty}}(t)$, we calculate the discrete Fourier transform a_j ($j = -N/2, \dots, N/2 - 1$) defined by

$$a_j = \sum_{k=0}^{N-1} G(t_k) e^{2\pi i f_j t_k} \quad (22)$$

where N is the total number of sampling points in the time-span ΔT , and $t_k = k\Delta T/N$ and $f_j = j/\Delta T$, and $|a_j| = |a_{-j}|$ for a real

function $G(t)$. To indicate the amplitude of the light variation with the frequency f_j , we use the quantity defined by

$$A(\omega_j) = 2|a_j|/N, \quad (23)$$

where $\omega_j = 2\pi f_j$.

3 NUMERICAL RESULTS

The surface r modes propagating in the fluid ocean of a rotating neutron star may be classified in terms of three quantum numbers (m, k, n), where m is the azimuthal wavenumber around the rotation axis, k is the number of latitudinal nodes, and n is the number of radial nodes of the eigenfunctions. For the quantum number k , we count the latitudinal nodes of the eigenfunctions $\text{Re}[\delta T(R, \theta)]$, and for the quantum number n we count the radial nodes of the eigenfunction $iT_{lj}(r)$. In this paper, we exclude the r modes of $l' = |m|$ for light-curve calculations, because their frequency changes during bursts are much larger than is suggested by observations (e.g. Cumming & Bildsten 2000; Lee 2004). Then, the r modes with the quantum number $k = 0, 1, 2, \dots$ respectively, and the corotating frame frequency ω decreases in this order for given m, n and Ω . The r modes with even k are denoted ‘even’ modes, and have eigenfunctions $\delta T(R, \theta)$ that are symmetric about the equator of the star, while the r modes with odd k are called ‘odd’ modes and are antisymmetric about the equator.

For light-curve calculations in this paper, we consider only the fundamental r modes with no radial nodes ($n = 0$) of the eigenfunction iT_{lj} , because they are the most strongly excited in thermonuclear bursts (Lee 2004). In addition, because the r modes associated with high m and k are unlikely to produce light variations with appreciable amplitudes, we restrict our numerical analysis to the fundamental modes with $m = 1$ or $m = 2$ and with $k = 0$ or $k = 1$. Employing these simplifications, and assuming two r modes with different m may be excited, we can express the surface temperature for light-curve calculation as

$$T(R, \theta, \phi, t) = T_0 + \text{Re} \left[C_1 \delta T^{\alpha_1}(R, \theta) e^{i(\phi + \sigma_{\alpha_1} t)} + C_2 e^{i\chi} \delta T^{\alpha_2}(R, \theta) e^{i(2\phi + \sigma_{\alpha_2} t)} \right], \quad (24)$$

where

$$\begin{aligned} \delta T^{\alpha_1}(R, \theta) &= \sum_{j \geq 1} \delta T_{lj}^{\alpha_1}(R) Y_{lj}^1(\theta, 0), \\ \delta T^{\alpha_2}(R, \theta) &= \sum_{j \geq 1} \delta T_{lj}^{\alpha_2}(R) Y_{lj}^2(\theta, 0), \end{aligned} \quad (25)$$

$C_1 = C_{\alpha_1}$ and $C_2 = C_{\alpha_2}$ are here real constants for the amplitudes of the modes, and χ is a real parameter, giving the phase difference between the two r modes. If we define $\alpha = (m, k, n)$, we have $\alpha_1 = (1, 0, 0)$ and $\alpha_2 = (2, 0, 0)$ for the even modes, and $\alpha_1 = (1, 1, 0)$ and $\alpha_2 = (2, 1, 0)$ for the odd modes. For the oscillation frequencies, we adopt the approximation that $\sigma_{\alpha_1} = -\Omega$ and $\sigma_{\alpha_2} = -2\Omega$. The parameters we need to calculate the function $G(t)$ defined by equation (9) are the mass M , the radius R , the angular rotation speed Ω of the star, the oscillation amplitudes C_1 and C_2 , the phase difference χ between the two modes, and the inclination angle i . For the function $G_{E_{\infty}}(t)$ defined by equation (8), we need in addition the surface temperature T_0 and the photon energy E_{∞} .

For the r -mode calculation, we use a mass-accreting envelope model with the rate $\dot{M} = 0.1 \dot{M}_{\text{Edd}}$ for a neutron star having $M = 1.4 M_{\odot}$ and $R = 10^6$ cm, where $\dot{M}_{\text{Edd}} = 4\pi c R / \kappa_e$ with κ_e being the electron scattering opacity. This envelope model is a fully radiative model with no convective regions in it, and the detail of the

Table 1. Oscillation frequencies $\bar{\omega}$ and $\bar{\sigma}/m$ for the fundamental ($n = 0$) r modes for the mass-accreting envelope model with $\dot{M} = 0.1\dot{M}_{\text{Edd}}$ for $M = 1.4 M_{\odot}$ and $R = 10$ km. Here the frequencies $\bar{\omega}$, $\bar{\sigma}$ and $\bar{\Omega}$ are normalized by $\sqrt{GM/R^3}$.

k	m	$\bar{\Omega} = 0.2$		$\bar{\Omega} = 0.4$	
		$\bar{\omega}$	$\bar{\sigma}/m$	$\bar{\omega}$	$\bar{\sigma}/m$
0	1	5.31(−3)	−0.1947	5.31(−3)	−0.3947
	2	1.02(−2)	−0.1949	1.04(−2)	−0.3948
1	1	3.24(−3)	−0.1968	3.22(−3)	−0.3967
	2	6.32(−3)	−0.1968	6.36(−3)	−0.3968

envelope calculation is given in Strohmayer & Lee (1996) and Lee (2004). To calculate the modes propagating in the mass-accreting envelope of a rotating neutron star, we follow the method described by Lee & Saio (1987, 1993), which is a fully non-adiabatic method and makes it possible to obtain the temperature variation δT itself as well as the relation between the temperature variation and the displacement vector components. Note that the formulation employed for the envelope and oscillation mode calculations is Newtonian, and no general relativistic effects are included. In Table 1, the oscillation frequencies $\bar{\omega}$ and $\bar{\sigma}/m$ are tabulated for the fundamental r modes with low m and k for $\bar{\Omega} = 0.2$ and $\bar{\Omega} = 0.4$, where the frequencies $\bar{\omega}$, $\bar{\sigma}$ and $\bar{\Omega}$ are normalized frequencies by $\sqrt{GM/R^3}$. For $M = 1.4 M_{\odot}$ and $R = 10$ km, we have $\omega/2\pi = 686\bar{\omega}$ Hz. For the r mode with $(k, m) = (0, 1)$ in Table 1, for example, we obtain $\omega/2\pi = 3.64$ Hz, the value of which is smaller by a factor of 2–3

than the estimation given by Piro & Bildsten (2005). This difference may be because we assume a steadily mass-accreting envelope whose temperature is lower than the temperature assumed in Piro & Bildsten (2005). It is important to note that the corotating frame oscillation frequency $\bar{\omega}$ is almost insensitive to $\bar{\Omega}$ for rapidly rotating stars (Lee 2004), and that for a given k the inertial frame pattern speed $\bar{\sigma}/m$ for $m = 2$ is nearly equal to that for $m = 1$, which may justify the simplification of $\sigma = -m\Omega$. The temperature variations $\delta T(R, \theta)/T_0$ caused by the surface r modes for $\bar{\Omega} = 0.2$ are shown in Fig. 2, where Figs 2(a)–(d) are for $\alpha = (1, 0, 0)$, $(2, 0, 0)$, $(1, 1, 0)$ and $(2, 1, 0)$, respectively, and the solid and dashed lines denote the real and imaginary parts, respectively, of the function $\delta T(R, \theta)/T_0$. Here, the amplitude normalization is given by $|\text{Re}[iT_{l_1}(R)/R]| = 1$ at the surface of the star. We note that the functions $\delta T(R, \theta)/T_0$ and $iT_{l_1}(R)/R$ have comparable amplitudes to each other at the stellar surface, and that the imaginary part of $\delta T(R, \theta)/T_0$ is much smaller than the real part. Heyl (2004) employed the normalization of the mode so that the effective temperature varies over the surface from zero to twice the underlying value. This normalization corresponds to the amplitudes of the horizontal displacement comparable to the radius of the star. For the light-curve calculations in this paper, for simplicity, we exclusively use $C_j = 0.2$, corresponding to $iT_{l_1}(R)/R = 0.2$ (see also the next paragraph). The θ dependence of the function $\delta T(R, \theta)/T_0$ for the even (odd) r mode with $m = 1$ is quite similar to that for the even (odd) r mode with $m = 2$ except for the fact that the maxima of the functions for $m = 2$ are larger than those for $m = 1$. In this paper, the temperature perturbations $\delta T(R, \theta)$ calculated for $R = 10$ km will be used for different values

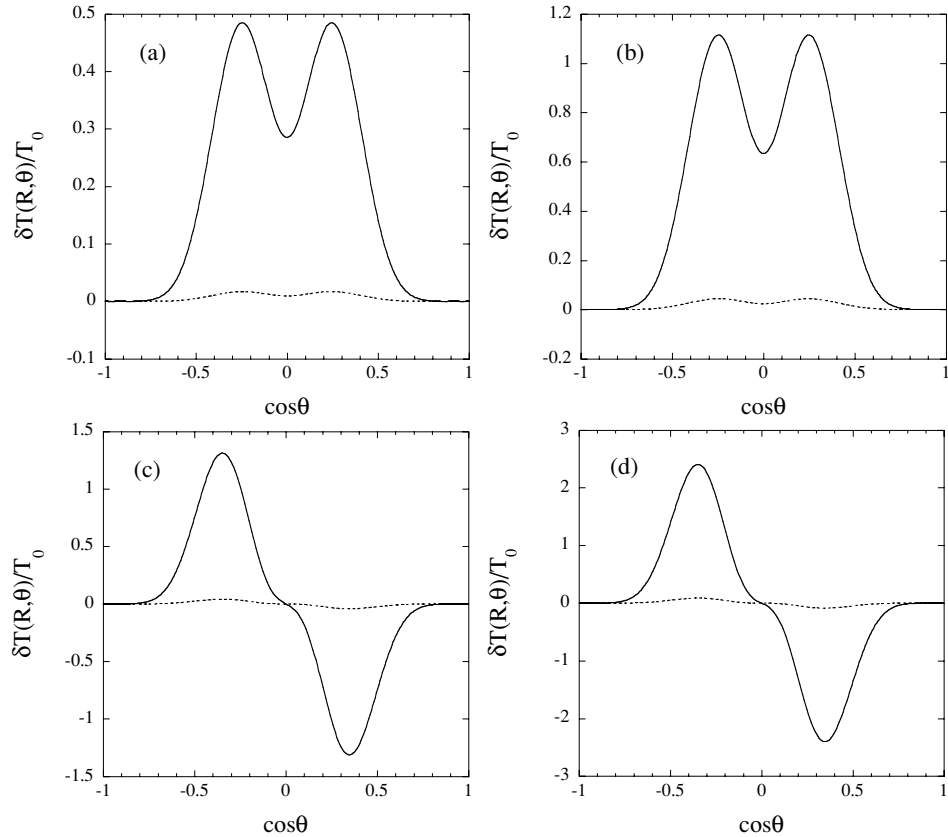


Figure 2. $\delta T(R, \theta)/T_0$ as a function of $\cos \theta$ for $\bar{\Omega} = 0.2$: (a) for the fundamental even r mode with $m = 1$; (b) for the fundamental even r mode with $m = 2$; (c) for the fundamental odd r mode with $m = 1$; (d) for the fundamental odd r mode with $m = 2$, where the solid and dotted lines indicate the real and the imaginary parts, respectively. Here, the amplitude normalization for the mode is given by $|\text{Re}[iT_{l_1}(R)/R]| = 1$ at the surface.

of R for simplicity. Applying the approximation $\sigma = -m\Omega$, we have $m\phi + \sigma_\alpha t = m\phi - m\Omega t$, and we call the Fourier amplitudes $A(\omega_j)$ at $\omega_j = \Omega$ and $\omega_j = 2\Omega$ the fundamental and the first harmonic components, respectively.

Because we are applying a linear theory of stellar pulsations, we cannot self-consistently determine the amplitudes of the modes, which forces us to treat the oscillation amplitudes as parameters in the modelling. For simplicity, we use $C_1 = 0.2$ for $m = 1$ and $C_2 = 0.2$ for $m = 2$ for the mode amplitudes throughout the following calculations. Because the toroidal component of the displacement vector is dominant for the r modes, the velocity, v , of a surface fluid element may be approximately given by $v \sim |\omega T_l(R)| = R\sqrt{GM/R^3}|\bar{\omega}| \times |iT_l(R)/R|$. Because $|\bar{\omega}| \lesssim 0.01$, we have the fluid velocity $v \lesssim 10^{-3} c$ for $|iT_l(R)/R| \sim 0.2$ if we adopt the stellar parameters $M = 1.4 M_\odot$ and $R = 10$ km, for which $R\sqrt{GM/R^3} \sim 0.5c$. If we use the sound velocity $v_s = k_B T / \mu H$ at the surface, we have $v_s \sim 10^{-3} c$ for $T = 10^7$ K and $\mu = 0.5$, where H and μ denote the hydrogen mass and the mean molecular weight, respectively. For the value of $C_1 = 0.2$ (or $C_2 = 0.2$) for the amplitude parameter, the fluid velocity at the surface is much smaller than the velocity of light and is comparable to or less than the local sound velocity at the surface.

3.1 Light curves produced by a single r mode with low m

Because the imaginary part of $\delta T(R, \theta)/T_0$ is much smaller than the real part, assuming that only a single r mode of low m is excited, we may simply write the surface temperature as

$$T = T_0 [1 + C(\theta) \cos(m\phi - m\Omega t)], \quad (26)$$

where $C(\theta) = \text{Re}[C_j \delta T(R, \theta)/T_0]$ and $j = 1$ or $j = 2$. Note that setting the origins of times t and t_∞ appropriately, we can assume $\Omega t = \Omega_\infty t_\infty$. The function $G(t)$ is given by

$$G(t) = G_0 + G_1^c \cos m\Omega t + G_1^s \sin m\Omega t + G_2^c \cos 2m\Omega t + G_2^s \sin 2m\Omega t + \dots, \quad (27)$$

where

$$G_0 = \int_0^1 2q dq \int_0^{2\pi} \frac{d\phi'}{2\pi} \frac{1 + 1.5C^2(\theta)}{f^3}, \quad (28)$$

$$G_1^c = \int_0^1 2q dq \int_0^{2\pi} \frac{d\phi'}{2\pi} 3f^{-3} C(\theta) \left[1 + \frac{C^2(\theta)}{4} \right] \times \cos m(\phi + \Delta\phi), \quad (29)$$

$$G_1^s = \int_0^1 2q dq \int_0^{2\pi} \frac{d\phi'}{2\pi} 3f^{-3} C(\theta) \left[1 + \frac{C^2(\theta)}{4} \right] \times \sin m(\phi + \Delta\phi), \quad (30)$$

$$G_2^c = \int_0^1 2q dq \int_0^{2\pi} \frac{d\phi'}{2\pi} \frac{3}{2} f^{-3} C^2(\theta) \cos 2m(\phi + \Delta\phi), \quad (31)$$

$$G_2^s = \int_0^1 2q dq \int_0^{2\pi} \frac{d\phi'}{2\pi} \frac{3}{2} f^{-3} C^2(\theta) \sin 2m(\phi + \Delta\phi). \quad (32)$$

Here, $\Delta\phi = \Omega_\infty \Delta t_\infty(b)$, and we have replaced t_∞ by $t_\infty - \Delta t_\infty(b)$ to calculate the light curves at t_∞ at the observer. It may be important to note that the coefficients G_1^s and G_2^s vanish if we assume $f = 1$ and $\Delta\phi = 0$. Equation (27) indicates that there appears a periodic component having the frequency $2m\Omega$ unless G_2^c and G_2^s vanish

simultaneously. The terms associated with the frequency $m\Omega$, for example, can be rewritten as

$$G_1^c \cos m\Omega t + G_1^s \sin m\Omega t = G_1 \cos(m\Omega t - \delta), \quad (33)$$

where $G_1 = \sqrt{(G_1^c)^2 + (G_1^s)^2}$, $\tan \delta = G_1^s/G_1^c$, and the value of $\Omega t = (\delta + 2n\pi)/m$ that maximizes the variation depends on the parameters R and i , where n is an integer. Because the imaginary part of $\delta T(T, \theta)$ is negligible compared with the real part, we have in a good approximation

$$A(m\Omega) = G_1, \quad A(2m\Omega) = G_2, \quad (34)$$

where $G_2 = \sqrt{(G_2^c)^2 + (G_2^s)^2}$, and the Fourier amplitude $A(\omega_j)$ is defined by equation (23). If we define the phase shift δ_j , using the Fourier transform a_j given in equation (22), as

$$\tan \delta_j = \text{Im}(a_j)/\text{Re}(a_j), \quad (35)$$

we have to good approximation $\delta = \delta_j$, selecting the integer j so that $2\pi f_j = m\Omega$.

The quantities G_1 and $\delta/(2m\pi)$ defined by equation (33) are plotted as a function of the inclination angle i for the even ($k=0$) r mode with $m=1$ in Fig. 3, and for the even ($k=0$) r mode with $m=2$ in Fig. 4, where we assume $\bar{\Omega} = 0.2$, and the dotted, short-dashed, solid, long-dashed and dot-dashed lines indicate the radii $R = 8, 9, 10, 15$ and 20 km, respectively. The amplitude G_1 vanishes at $i = 0$ because the temperature variations are proportional to $e^{im\phi}$ where $\phi = \phi'$ for $i = 0$. For given i and R , the amplitude G_1 for $m=1$ is usually larger than that for $m=2$. For a given inclination angle i , the amplitude $A(m\Omega) = G_1$ decreases as the radius R decreases. This is because the maximum angle θ'_{\max} increases with decreasing R so that almost the whole surface area of the star can be seen at any time by the distant observer. For the even modes, the amplitude G_1 for a given R monotonically increases with increasing i . As shown by Figs 3 and 4, the phase shifts $\delta/(2m\pi)$ for the even r modes are negative. The absolute value $|\delta/(2m\pi)|$ for $m=1$, which remains small, increases with decreasing R , and it is rather insensitive to the inclination angle i for a given R . The absolute value $|\delta/(2m\pi)|$ for $m=2$ also increases as R decreases and becomes as large as $|\delta/(2m\pi)| \sim 0.2$ for the smallest R considered here. It shows a weak dependence on i , particularly for the radii $R \sim 10$ km.

The quantities G_1 and $\delta/(2m\pi)$ are given as a function of the inclination angle i for the odd ($k=1$) r mode with $m=1$ in Fig. 5, and for the odd ($k=1$) r mode with $m=2$ in Fig. 6, where $\bar{\Omega} = 0.2$, and the different curves have the same meaning as in Fig. 3. For the odd modes, the amplitude G_1 vanishes at $i = 90^\circ$ also, because the temperature variation pattern is antisymmetric about the equator of the star. As in the case of the even r modes, the amplitude G_1 for the odd r modes decreases with decreasing R for a given i . Although $\delta/(2m\pi)$ for larger radii $R \gtrsim 15$ km remains constant with varying i , it shows a strong dependence on i for smaller radii $R \lesssim 10$ km.

Fig. 7 shows the amplitude ratio G_2/G_1 for the even r mode with $m=1$ (upper panel) and for the odd r mode with $m=1$ (lower panel) as a function of i . We find the ratio is at most of the order of ~ 0.01 for the even $m=1$ r modes, which indicates that the first harmonic component cannot be significant in the light curves produced by a single even r mode of low m . For the odd $m=1$ r mode, on the other hand, the first harmonic component has appreciable amplitude compared to the fundamental, particularly when $i \sim 90^\circ$. Actually, the ratio G_2/G_1 diverges as i increases to 90° .

As examples, we show as a function of $\Omega t/2\pi$ the light curves produced by the even, $m=1$ r mode in Fig. 8, and by the odd, $m=1$ r mode in Fig. 9, where we assume $\bar{\Omega} = 0.2$ and $i = 60^\circ$. Fig. 10 shows the light curves generated by the odd, $m=1$ r mode as a

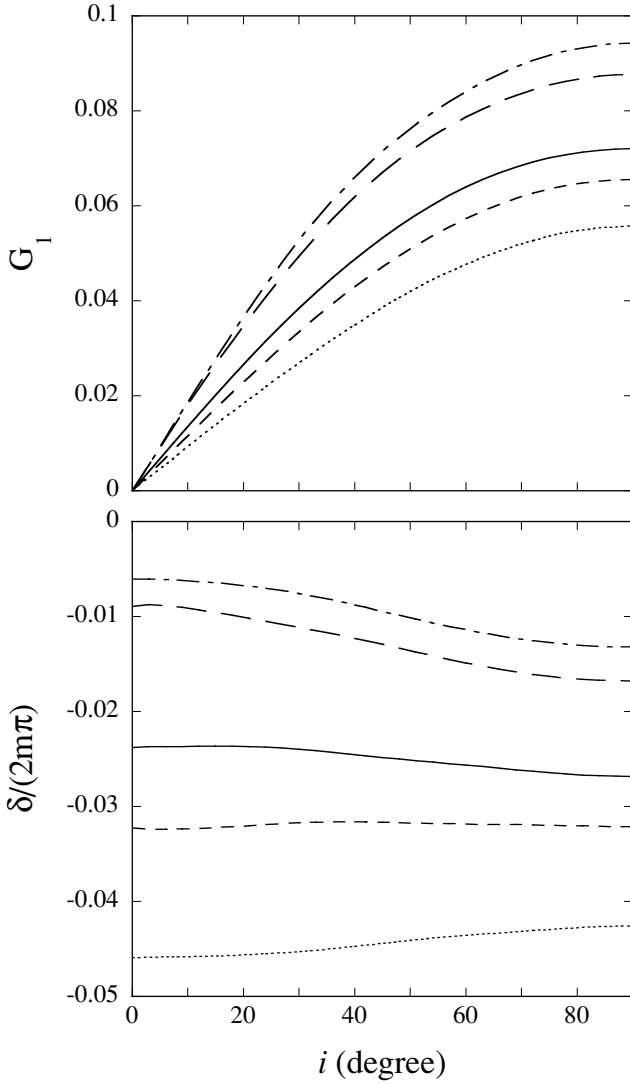


Figure 3. Amplitude G_1 and phase shift δ as a function of the inclination angle i for the fundamental even r mode with $m = 1$ ($C_1 = 0.2$, $C_2 = 0$ and $\chi = 0$), where $\bar{\Omega} = 0.2$, and the dotted, short-dashed, solid, long-dashed and dash-dotted lines are for the radii $R = 8, 9, 10, 15$ and 20 km, respectively. Here, the amplitude normalization for the mode is given by $|\text{Re}[iT_{l_1}(R)/R]| = 1$ at the surface.

function of $\Omega t/2\pi$ for $\bar{\Omega} = 0.2$ and $R = 10$ km, where the dotted, short-dashed, solid, long-dashed and dot-dashed lines indicate the inclination angles $i = 10^\circ, 30^\circ, 50^\circ, 70^\circ$ and 90° , respectively. At $i = 90^\circ$, only the first harmonic component associated with $2m\Omega$ appears.

3.2 Dependence on $\bar{\Omega}$

As Ω increases, the amplitudes of the r modes are more strongly confined to the equatorial region of the star, which makes the amplitude G_1 larger for the even r modes but smaller for the odd modes. Note that the frequency ω is only weakly dependent on Ω for the modes. To see the effects of rapid rotation, we calculate G_1 and δ for the even, $m = 1$ r mode for $\bar{\Omega} = 0.4$, and we plot the results in Fig. 11, where the different curves represent different radii as in Fig. 3. We note that the magnitude of the phase shift δ is larger for

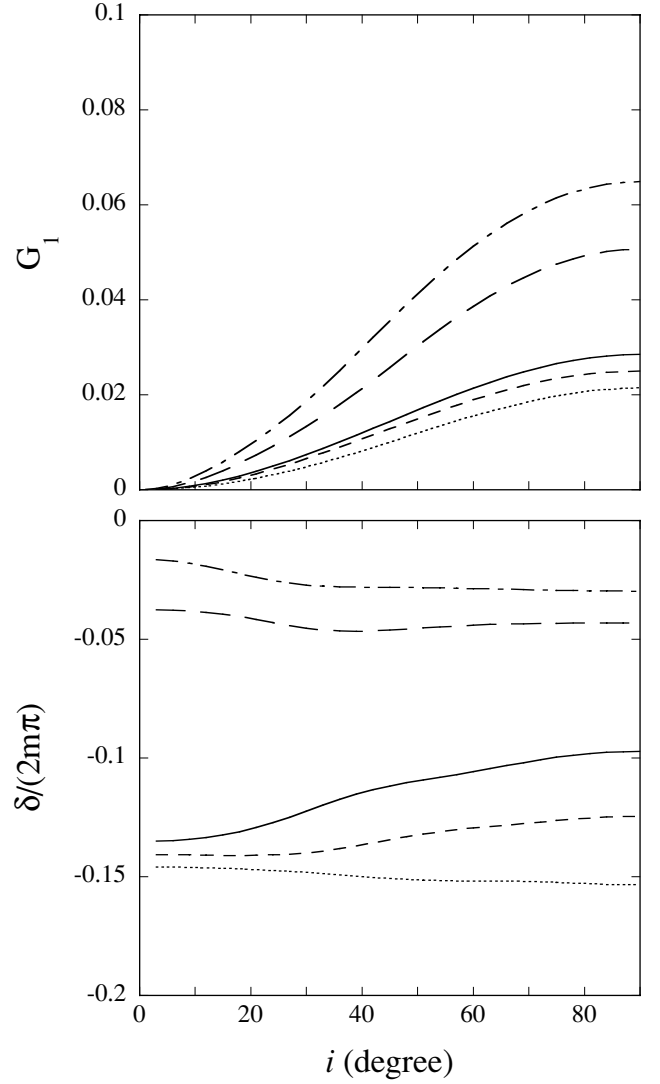


Figure 4. Same as Fig. 3 but for the fundamental even r mode with $m = 2$ ($C_1 = 0$, $C_2 = 0.2$ and $\chi = 0$).

$\bar{\Omega} = 0.4$ than for $\bar{\Omega} = 0.2$ although δ is still only weakly dependent on the inclination angle i for the mode.

3.3 Light curves produced by two r modes

Although the even, $m = 1$ r mode will produce the largest light variations of the modes considered here, the mode is not likely to produce a first harmonic component $A(2\Omega)$ of appreciable strength. In order to account for observed light curves that contain a substantial first harmonic component, we may need to assume that the r modes with $m = 1$ and $m = 2$ are excited simultaneously. As an example, we calculate the light curves $G(t)$ produced by the two simultaneously excited even r modes with $m = 1$ and $m = 2$, assuming $C_1 = C_2 = 0.2$, $\chi = 0$, $i = 90^\circ$ and $\bar{\Omega} = 0.2$. We plot $G(t)$ as a function of $\Omega t/2\pi$ in Fig. 12 and the Fourier amplitudes $A(\Omega)$ and $A(2\Omega)$ as a function of the radius R in Fig. 13, where the different curves in Fig. 12 have the same meaning as in Fig. 3. Obviously, using two r modes with different m , we can produce a variety of light curves, including those with a harmonic content similar to that seen from XTE J1814–338 (Strohmayer et al. 2003). It is important to note

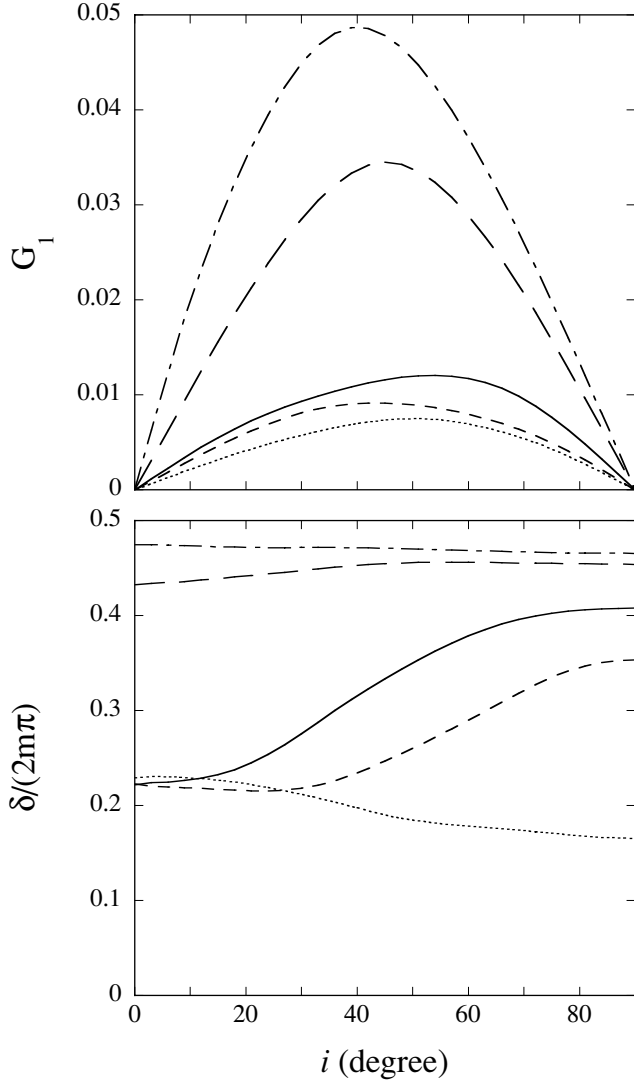


Figure 5. Same as Fig. 3 but for the fundamental odd r mode with $m = 1$ ($C_1 = 0.2$, $C_2 = 0$ and $\chi = 0$).

that, even if we abandon the simplification given by $\sigma_{\alpha_1} = -\Omega$ and $\sigma_{\alpha_2} = -2\Omega$, we have in a good approximation $2\sigma_{\alpha_1} = \sigma_{\alpha_2}$ as shown by Table 1.

3.4 Phase lags

The amplitudes of the light curves produced by the surface r modes are inevitably related to the parameters C_i as well as to the ratio R/M . Because the oscillation amplitudes are difficult to determine within the framework of a linear theory of stellar pulsations and the ratio R/M itself is one of our main parameters to determine observationally, it would be useful to find an additional observable that can be used as an indicator for the ratio R/M . Considering the even r mode with $m = 1$, which is most likely to be responsible for the light variations, we note that the phase shift δ , which is almost independent of the oscillation amplitude parameter C_1 , is rather insensitive to the inclination angle i but is almost a monotonic function of the radius R (i.e. the ratio R/M) for a given i . If it is true that the observed light variations during burst oscillations are caused by an even, $m = 1$ r mode, it would be possible to use the phase shift δ as an

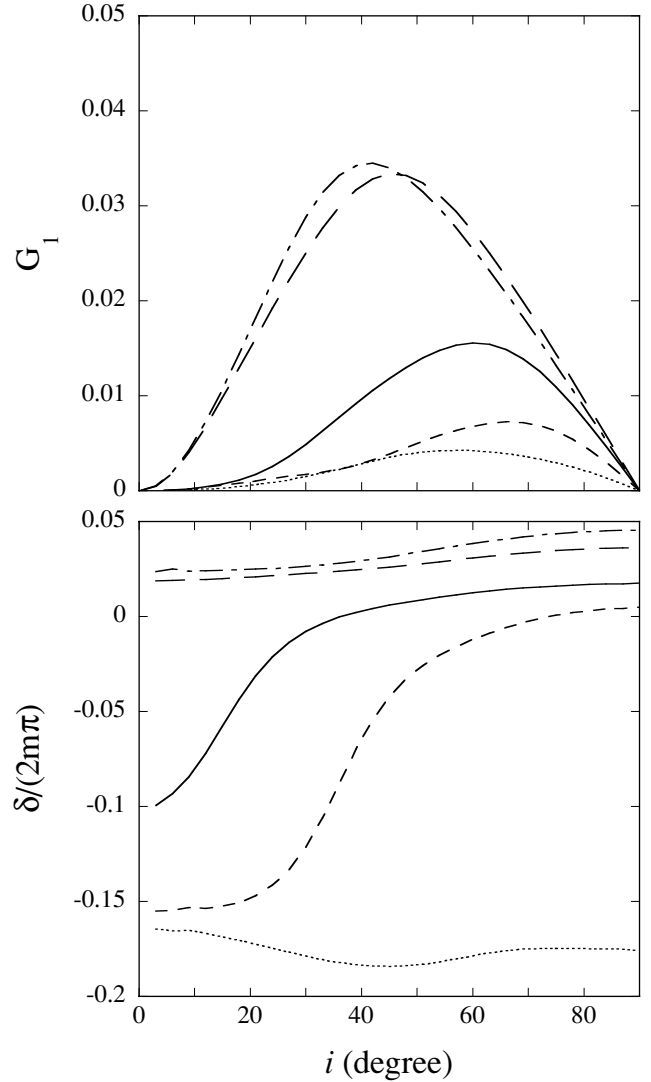


Figure 6. Same as Fig. 3 but for the fundamental odd r mode with $m = 2$ ($C_1 = 0$, $C_2 = 0.2$ and $\chi = 0$).

indicator for the ratio R/M . To derive an observable using the phase shift δ , we calculate the function $G_{E_\infty}(t)$ defined in equation (8) for appropriate values of T_0 and E_∞ , and Fourier analyse the function $G_{E_\infty}(t)$ to obtain the phase shift δ_j at $\omega_j = \Omega$ using equation (35), which we denote δ_E . In Fig. 14, we plot as a function of the inclination angle i the difference $\delta - \delta_{E_0}$ for the even, $m = 1$ r mode (upper panel) and for the odd, $m = 1$ r mode (lower panel) where we have assumed $\bar{\Omega} = 0.2$, $E_\infty = E_0 = 1$ keV, $k_B T_0 = 2.3$ keV, and the various curves represent different radii as in Fig. 3. Because the difference $\delta - \delta_{E_0}$ for the even r mode with $m = 1$ is almost insensitive to i and its magnitude increases almost monotonically with the radius R for a given i , the difference may be useful as an observational indicator for the ratio R/M . On the other hand, the difference for the odd mode shows a strong dependence on i for the radius $R \lesssim 10$ km. Because the phase shifts δ found in this paper are due mainly to the Doppler effects associated with rapid rotation of the star, the magnitude of the difference will be large for higher $\bar{\Omega}$ for given M and R .

As shown in Fig. 14, the phase difference, $\delta - \delta_{E_0}$, for the even mode is always negative, but that for the odd mode can be positive

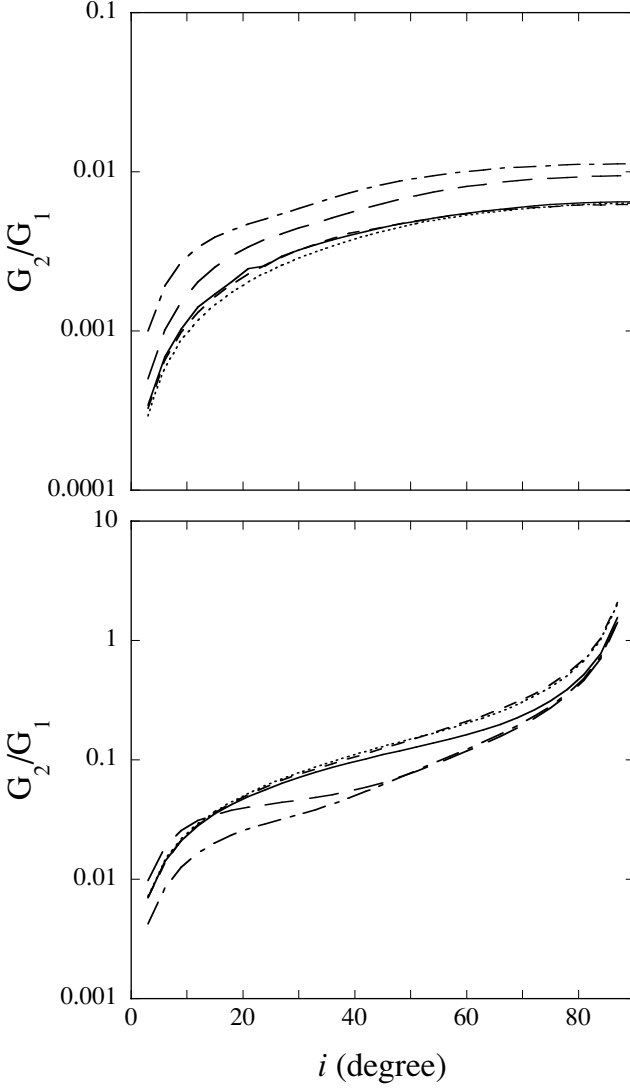


Figure 7. Ratio G_2/G_1 as a function of the inclination angle i for the fundamental even r mode with $m = 1$ (upper panel) and for the fundamental odd r mode with $m = 1$ (lower panel), where $\bar{\Omega} = 0.2$, and the various curves represent different radii as in Fig. 3. Here, the amplitude normalization for the mode is given by $|\text{Re}[iT_{l_1}(R)/R]| = 1$ at the surface.

for radii $R \lesssim 10$ km. Here, negative and positive values of $\delta - \delta_{E_0}$ indicate hard leads and lags, respectively, for $E_\infty = E_0 = 1$ keV and $k_B T_0 = 2.3$ keV. To compare with observations more directly, it is convenient to give the phase shift difference, $\delta_E - \delta_{E_0}$, between the phase for $E_\infty = E$ and that for a particular $E_\infty = E_0$. Examples are given as a function of the photon energy E in Fig. 15 for the even r mode with $m = 1$ for $i = 60^\circ$ and in Fig. 16 for the odd r mode with $m = 1$ for $i = 30^\circ$ (upper panel) and for $i = 60^\circ$ (lower panel), where we have used $E_0 = 1$ keV and $\Omega_\infty/2\pi = 400$ Hz. For the even mode we always have negative $\delta_E - \delta_{E_0}$, indicating hard leads (soft lags), as suggested by Fig. 14. On the other hand, for the odd $m = 1$ r mode, we have both hard leads (soft lags) and hard lags, the latter of which occur at smaller radii (i.e. smaller R/M). Observationally, there is an indication for hard lags during some burst oscillations; however, others are consistent with no phase variations with energy (Muno et al. 2003). Because the even, $m = 1$ r mode generates hard leads (as the hotspot model does), our

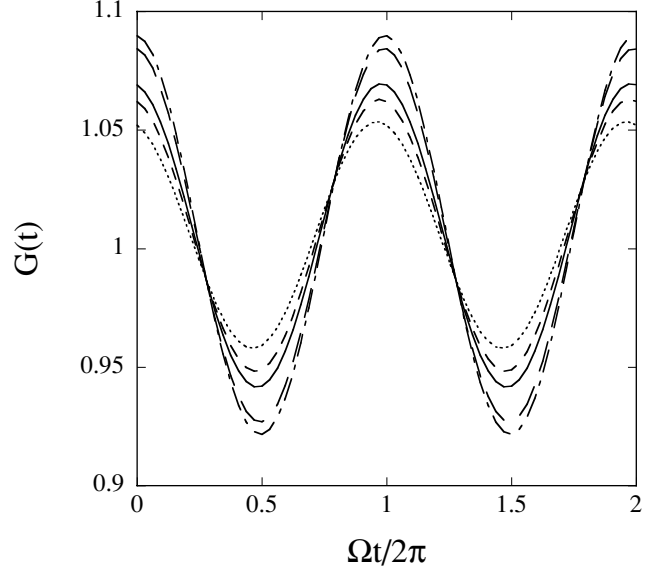


Figure 8. $G(t)$ as a function of $\Omega t/2\pi$ for the fundamental even r mode with $m = 1$ for $i = 60^\circ$, where $C_1 = 0.2$, $C_2 = 0$, $\chi = 0$ and $\bar{\Omega} = 0.2$, and the various curves represent different radii as in Fig. 3. Here, the amplitude normalization for the mode is given by $|\text{Re}[iT_{l_1}(R)/R]| = 1$ at the surface.

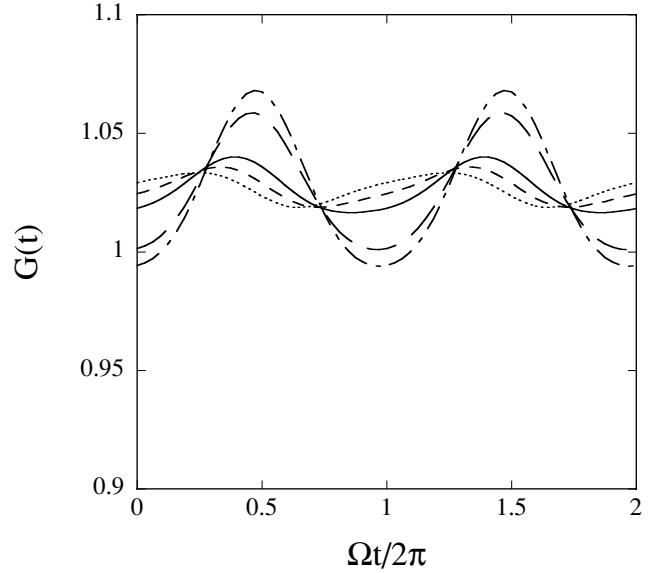


Figure 9. Same as Fig. 8 but for the fundamental odd r mode with $m = 1$.

results suggest that a single even r mode is probably inconsistent with burst oscillations which show hard lags. However, it might be possible for an oscillation produced by contributions from both even and odd modes to match the observed phase lag properties of burst oscillations. We will explore detailed modelling and fitting, including the effects of the detection process, in a subsequent paper.

4 DISCUSSION

Let us first in this section give an analytical discussion of the latitudinal dependence of the eigenfunctions for the surface r modes, following Pedlosky (1987). We also give in the next paragraph

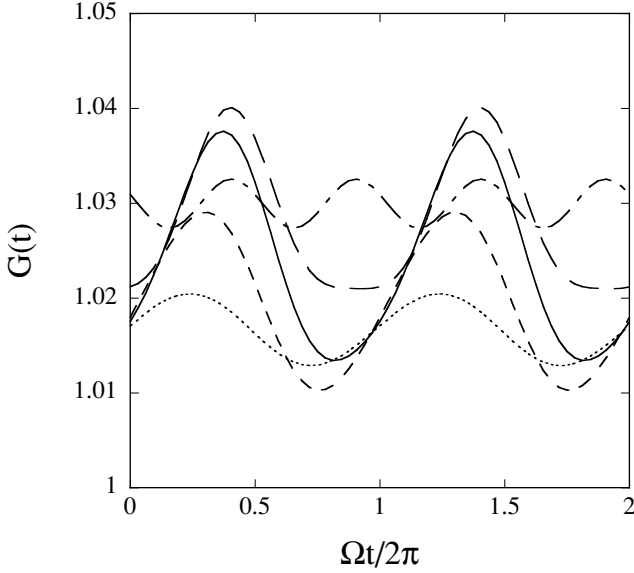


Figure 10. $G(t)$ as a function of $\Omega t/2\pi$ for the fundamental odd r mode with $m = 1$ for $R = 10$ km, where $C_1 = 0.2$, $C_2 = 0$, $\chi = 0$ and $\bar{\Omega} = 0.2$, and the dotted, short-dashed, solid, long-dashed and dash-dotted lines indicate the inclination angles $i = 10^\circ, 30^\circ, 50^\circ, 70^\circ$ and 90° , respectively. Here, the amplitude normalization for the mode is given by $|\text{Re}[iT_{l_1}(R)/R]| = 1$ at the surface.

an estimate of the amount of energy necessary to excite a surface r mode to observable amplitudes. The surface r modes considered in this paper belong to a subclass of the equatorial waves (Pedlosky 1987). In the equatorial β plane approximation, we employ a Cartesian coordinate system in which the coordinate origin is at the equator and the x -, y - and z -axes are in the eastward, northward and upward directions, respectively. The wave equations in the β plane approximation are solved by applying the method of separation of variables, in which a separation constant λ is introduced between (x, y, t) and z . The separation constant λ is an eigenvalue that is determined by solving the wave equation in the vertical direction with appropriate boundary conditions, and reflects the vertical structure of the thin fluid envelope. Assuming the perturbed velocity $v'_y(x, y, z, t)$ is given by $v'_y \propto e^{i(kx + \omega t)} \Psi(y)V(z)$, we obtain for the equatorial waves the dispersion relation given by (Pedlosky 1987)

$$\lambda \bar{\omega}^2 + \tilde{k}/\bar{\omega} - \tilde{k}^2 = (2j + 1)\sqrt{\lambda}, \quad (36)$$

where

$$\begin{aligned} \bar{\omega} &= \omega/(\beta_0 L_e), & \tilde{k} &= L_e k, \\ L_e &= \sqrt{N_0 D/\beta_0}, & \beta_0 &= 2\Omega/R. \end{aligned} \quad (37)$$

Here, N_0 is a characteristic value of the Brunt-Väisälä frequency, D is the depth of the fluid ocean, and the function $\Psi(y)$ is given by

$$\Psi(y) = \psi_j(\tau) \equiv e^{-\tau^2/2} H_j(\tau) / \sqrt{2^j j! \pi^{1/2}}, \quad (38)$$

where $H_j(\tau)$ is the Hermite polynomial, $\tau = \lambda^{1/4} y/L_e$, and j is an integer. Here, the function $V(z)$ is determined by the wave equation in the vertical direction. The pressure perturbation for the equatorial waves for $j \geq 1$ is then given by (Pedlosky 1987)

$$\begin{aligned} p'(x, y, z, t) = -\text{Re} \left\{ \frac{i A_j}{\lambda^{3/4}} \left[-\left(\frac{j}{2}\right)^{1/2} \frac{\psi_{j-1}(\tau)}{\bar{\omega} - \tilde{k}/\sqrt{\lambda}} \right. \right. \\ \left. \left. + \left(\frac{j+1}{2}\right)^{1/2} \frac{\psi_{j+1}(\tau)}{\bar{\omega} + \tilde{k}/\sqrt{\lambda}} \right] e^{i(kx + \omega t)} V(z) \right\}, \end{aligned} \quad (39)$$

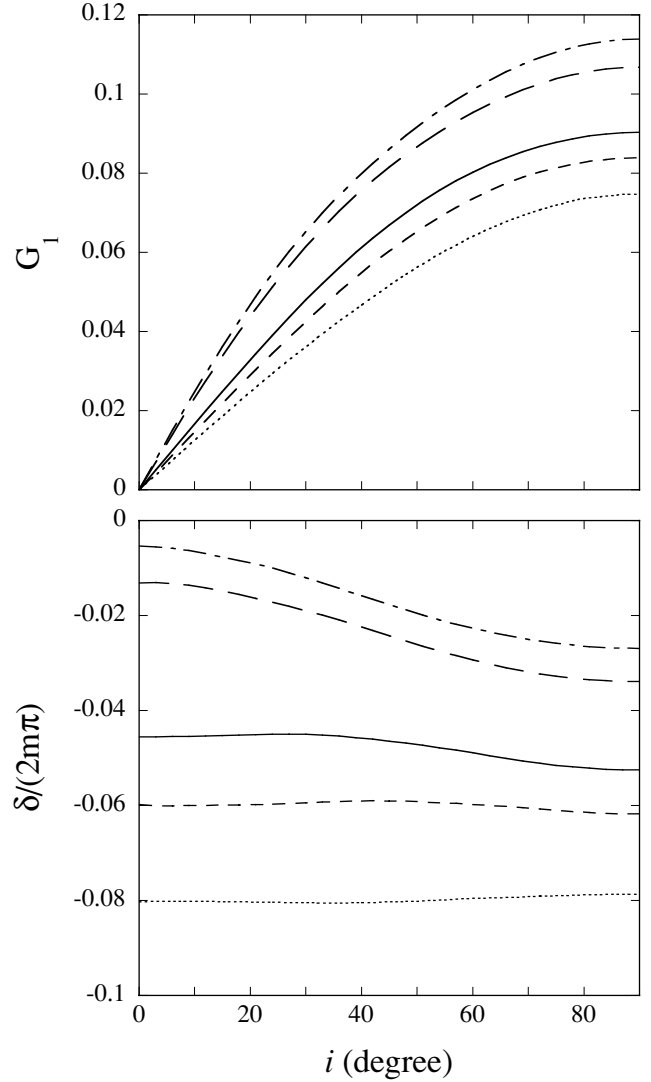


Figure 11. Same as Fig. 3 but for $\bar{\Omega} = 0.4$.

where A_j is an arbitrary constant. Because the low-frequency equatorial waves at rapid rotation have (Lee 2004)

$$\omega \sim \frac{m N_0 D / R}{(2j + 1)\sqrt{\lambda}}, \quad (40)$$

where we have assumed $k \sim m/R$, $p'(x, y, z, t)$ reduces to for $j = 1$

$$\begin{aligned} p'(x, y, z, t) \sim -\text{Re} \left[\frac{3}{2\sqrt{2}\pi^{1/4}} \frac{i A_1}{\lambda^{1/4} L_e k} \left(\tau^2 + \frac{1}{2} \right) \right. \\ \left. \times e^{-\tau^2/2} e^{i(kx + \omega t)} V(z) \right], \end{aligned} \quad (41)$$

and for $j = 2$

$$\begin{aligned} p'(x, y, z, t) \sim -\text{Re} \left[\frac{5}{3\sqrt{2}\pi^{1/4}} \frac{i A_2}{\lambda^{1/4} L_e k} \tau^3 e^{-\tau^2/2} \right. \\ \left. \times e^{i(kx + \omega t)} V(z) \right]. \end{aligned} \quad (42)$$

Knowing that the perturbed potential temperature Θ' is approximately given by $\Theta' = p'/z$ (Pedlosky 1987), we find that the latitudinal (y) dependence of $\Theta'(x, y, z, t)$ well reproduces that of

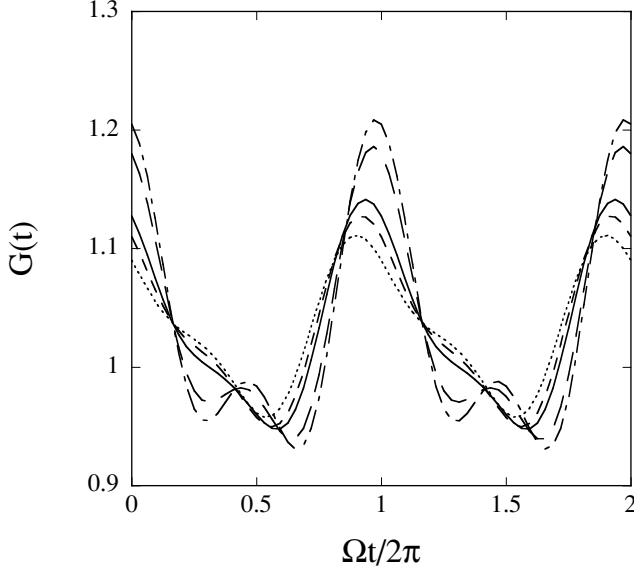


Figure 12. $G(t)$ as a function of $\Omega t/2\pi$ for the fundamental even r modes with $m = 1$ and $m = 2$ for $i = 90^\circ$, where $C_1 = C_2 = 0.2$, $\chi = 0$ and $\bar{\Omega} = 0.2$, and the various curves represent different radii as in Fig. 3. Here, the amplitude normalization for the mode is given by $|\text{Re}[i T_{l1}(R)/R]| = 1$ at the surface.

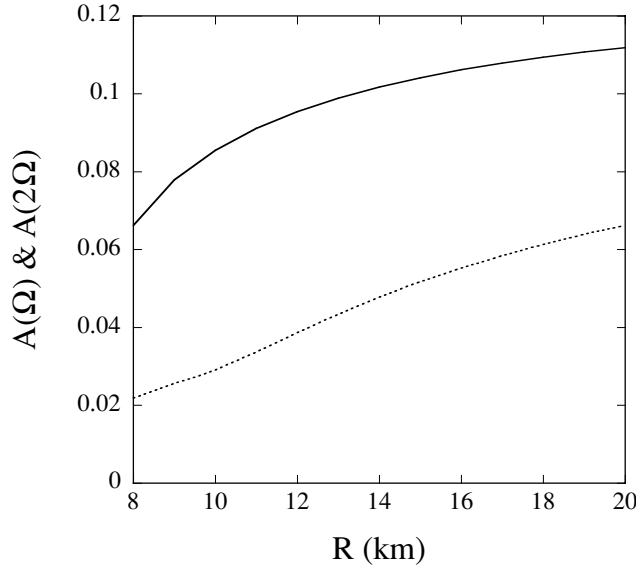


Figure 13. Fourier amplitudes $A(\Omega)$ and $A(2\Omega)$ as a function of the radius R for the fundamental even r modes with $m = 1$ and $m = 2$ for $i = 90^\circ$, where $C_1 = C_2 = 0.2$, $\chi = 0$ and $\bar{\Omega} = 0.2$, and the solid and dotted lines indicate $A(\Omega)$ and $A(2\Omega)$, respectively. Here, the amplitude normalization for the modes is given by $|\text{Re}[i T_{l1}(R)/R]| = 1$ at the surface.

$\delta T(R, \theta)/T_0$ in Fig. 2 both for the even r modes ($j = 1$) and for the odd r modes ($j = 2$). Note that the solutions having the frequency (40) correspond to the type 2 solutions discussed by Longuet-Higgins (1968).

The oscillation energy E_W of a mode observed in the corotating frame may be given by (e.g. Unno et al. 1989)

$$E_W = \frac{\omega^2}{2} \int_{\Delta M_e} \xi \cdot \xi^* dM_r = \bar{\omega}^2 \frac{GM \Delta M_o}{R}, \quad (43)$$

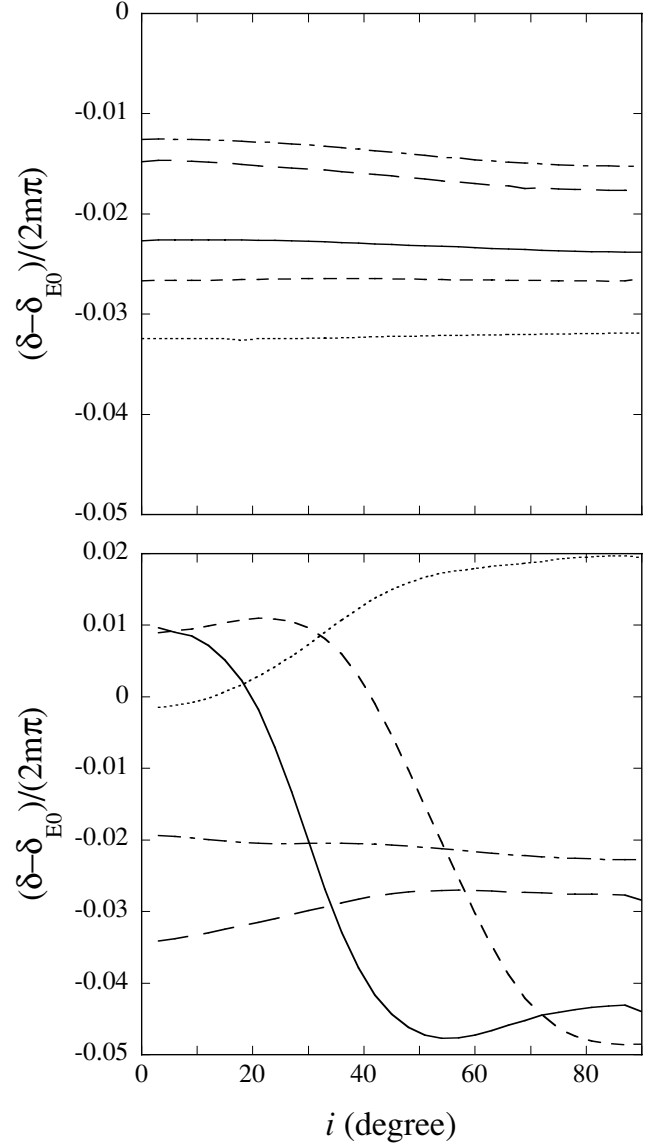


Figure 14. Phase shift difference $(\delta - \delta_{E_0})/(2m\pi)$ as a function of the inclination angle i for the fundamental even $m = 1$ r mode (upper panel) and for the fundamental odd $m = 1$ r mode (lower panel), where $\bar{\Omega} = 0.2$, $C_1 = 0.2$, $C_2 = 0$, and $\chi = 0$, and the various curves represent different radii as in Fig. 3. Here, we have assumed $k_B T_0 = 2.3$ keV and $E_\infty = E_0 = 1$ keV to calculate the function $G_{E_\infty}(t)$ and the phase shift δ_{E_0} . Negative values of $(\delta - \delta_{E_0})/(2m\pi)$ indicate hard leads.

where

$$\Delta M_o = \frac{1}{2} \int_{\Delta M_e} \frac{\xi \cdot \xi^*}{R^2} dM_r, \quad (44)$$

ξ^* is the complex conjugate of ξ , and ΔM_e is the envelope mass. If we let ΔE_b and ΔE_p denote the energies released during a burst and a persistent phase, respectively, we may assume $\alpha \equiv \Delta E_p/\Delta E_b \sim 10^2$ and $\Delta E_p \sim \epsilon GM \Delta M_a/R$, where $\epsilon \sim 0.1$ is a factor representing the efficiency of energy transformation from gravitational to radiation energies and $\Delta M_a = \dot{M} \Delta t_p$ with $\dot{M} \sim 10^{16} \text{ gs}^{-1}$ being a typical mass accretion rate found in low mass close binary systems is the amount of mass accreting during the persistent phase

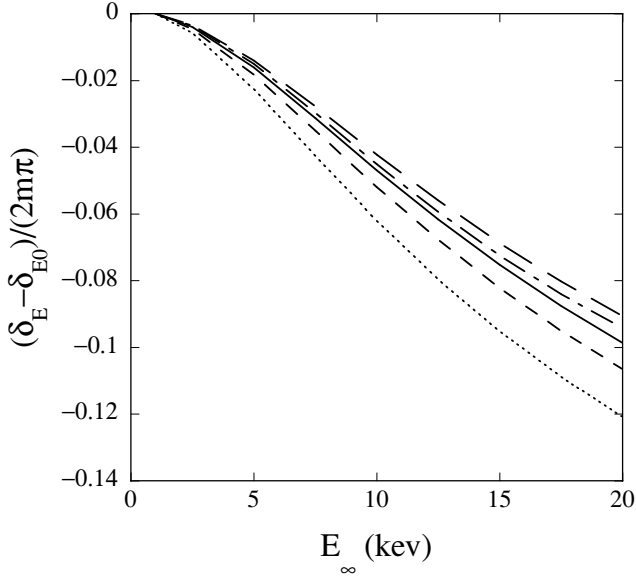


Figure 15. Phase shift difference $(\delta_E - \delta_{E_0})/(2m\pi)$ as a function of the photon energy $E_\infty = E$ for the fundamental even $m = 1$ r mode, where $\Omega_\infty/2\pi = 400$ Hz, $C_1 = 0.2$, $C_2 = 0$, $\chi = 0$ and $i = 60^\circ$, and the various curves represent different radii as in Fig. 3. Here, we have assumed $k_B T_0 = 2.3$ keV and $E_\infty = E_0 = 1$ keV to calculate the function $G_{E_\infty}(t)$ and the phase shift difference $(\delta_E - \delta_{E_0})/(2m\pi)$, the negative values of which indicate hard leads.

$\Delta t_p \sim 10^4$ s (see, e.g. Frank, King & Raine 2002). We then have

$$E_W = \alpha \epsilon^{-1} \bar{\omega}^2 (\Delta M_o / \Delta M_a) \Delta E_b, \quad (45)$$

which may be rewritten with appropriate normalization as

$$E_W \sim 2 \times \frac{\alpha}{100} \left(\frac{\epsilon}{0.1} \right)^{-1} \left(\frac{\dot{M}}{5 \times 10^{-18} M_\odot \text{s}^{-1}} \right)^{-1} \times \left(\frac{\Delta t_p}{10^4 \text{s}} \right)^{-1} \left(\frac{\bar{\omega}}{0.01} \right)^2 \left(\frac{C}{0.1} \right)^2 \frac{\langle \Delta M_o \rangle}{10^{-10} M_\odot} \Delta E_b, \quad (46)$$

where we have defined

$$\langle \Delta M_o \rangle = \frac{1}{2} \int_{\Delta M_e} \frac{\tilde{\xi} \cdot \tilde{\xi}^*}{R^2} dM_r, \quad (47)$$

assuming $\xi = C\tilde{\xi}$ with $\tilde{\xi}$ being the displacement vector normalized by $|\text{Re}[iI_l(R)/R]| = 1$. For the r modes discussed in this paper, we have the ratio $\langle \Delta M_o \rangle / 10^{-10} M_\odot \sim 0.1$ for the even r modes, and $\langle \Delta M_o \rangle / 10^{-10} M_\odot \sim 0.01$ for the odd r modes, for $\bar{\Omega} = 0.2$ and $\Delta M_e = 10^{-10} M_\odot$. Note that, although non-linear effects will be significant and produce strong harmonic components in observed light curves if the mode amplitudes become as large as $C \sim 1$, non-linear coupling with other modes will tend to saturate the mode amplitudes (e.g. Lindblom, Tohline & Vallisneri 2002; Arras et al. 2003). Although the estimation given above contains many parameters, all of which are not necessarily well determined, we may expect that the amount of energy required to excite the modes to appreciable amplitudes is a modest fraction of that released in a burst. It is interesting to note that, although the odd r modes need to have larger amplitudes to produce appreciable light variations than the even r modes, the former are easier to excite than the latter for a given amount of energy released in a burst.

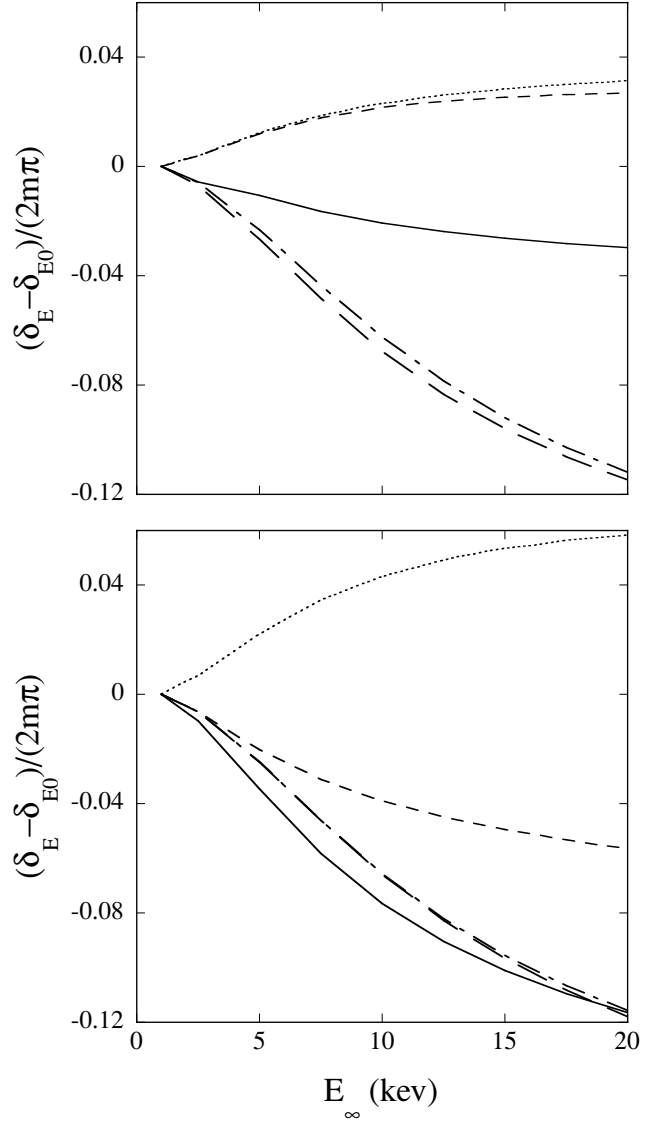


Figure 16. Phase shift difference $(\delta_E - \delta_{E_0})/(2m\pi)$ as a function of the photon energy $E_\infty = E$ for the fundamental odd $m = 1$ r mode for $i = 30^\circ$ (upper panel) and for $i = 60^\circ$ (lower panel), where $\Omega_\infty/2\pi = 400$ Hz, $C_1 = 0.2$, $C_2 = 0$ and $\chi = 0$, and the various curves represent different radii as in Fig. 3. Here, we have assumed $k_B T_0 = 2.3$ keV and $E_\infty = E_0 = 1$ keV to calculate the function $G_{E_\infty}(t)$ and the phase shift difference $(\delta_E - \delta_{E_0})/(2m\pi)$, the negative values of which indicate hard leads.

5 CONCLUSIONS

We have calculated light curves produced by the surface r modes of a rotating neutron star, taking account of the effects of gravitational light bending, gravitational redshift, and the difference in the arrival times of photons travelling in the static Schwarzschild space-time, as well as the Doppler shift of photon energy due to rapid spin of the star. We find that the fundamental even r mode with $m = 1$ produces the largest light variations. The light curves produced by a single even r mode of a given m are dominated by the fundamental component with frequency $m\Omega$, although those produced by a single odd r mode also contain a first harmonic component of appreciable amplitude as well as the fundamental component, the relative strengths depending on the inclination angle i . The phase shift $\delta - \delta_{E_0}$ produced by the even $m = 1$ r mode is only weakly dependent on the

inclination angle i and is almost a monotonic function of R for a given i . The phase shift produced by the even r mode with $m = 1$ is a hard lead. The phase shift produced by the odd, $m = 1$ r mode, on the other hand, depends both on i and on R , and there exists a parameter space of R and i which produces hard lags.

It is useful to translate the phase shift difference into a hard-lag measure, Δt_{Lag} , which is given for $\Omega_{\infty}/2\pi = 400$ Hz by

$$\Delta t_{\text{Lag}} = \frac{2\pi}{\Omega_{\infty}} \frac{\delta_E - \delta_{E_0}}{2m\pi} = 2.5 \frac{\delta_E - \delta_{E_0}}{2m\pi} \text{ ms}, \quad (48)$$

where negative Δt_{Lag} means hard leads. As indicated by Fig. 15, to fit the observed hard leads $\sim -200 \mu\text{s}$ at $E_{\infty} \sim 10$ keV for SAX J1808.4–3658 (Cui et al. 1998) in terms of the even $m = 1$ r mode we need slightly smaller values of the ratio R/R_G than the smallest value $R/R_G = 1.94$ for $M = 1.4 M_{\odot}$ and $R = 8$ km we use in this paper. In fact, Weinberg et al. (2001) have assumed $M = 2.2 M_{\odot}$ and $R = 10$ km for their fit, which is equivalent to $R/R_G = 1.54$, the value of which is substantially smaller than $R/R_G = 1.94$. As suggested by Fig. 16, however, the phase shift difference produced by the odd $m = 1$ r mode may give a consistent value $\sim -200 \mu\text{s}$ at $E_{\infty} \sim 10$ keV for $M = 1.4 M_{\odot}$, $R = 10$ km, and $i = 60^\circ$, although the strong saturation of Δt_{Lag} above $E \gtrsim 10$ keV is not necessarily well reproduced.

Heyl (2005) have carried out a similar calculation of light curves produced by the even r mode with $l' = 2$ and $m = 1$, using the formalism by Chen & Shaham (1989), and assuming the surface temperature is proportional to a uniform component plus a component proportional to the local amplitude of the r mode, given in Longuet-Higgins (1968). Heyl (2005) obtained quite similar results to ours, showing low harmonic contents and hard leads in the light curves. He has also shown that the pulsed fraction increases with increasing photon energy, which is also indicated by Fig. 17, where the Fourier amplitudes $A(\Omega)$ (solid lines) and $A(2\Omega)$ (dotted lines) are plotted as a function of photon energy E_{∞} for the even r mode with $l' = 2$ and $m = 1$ and for the odd r mode with $l' = m = 1$ (filled

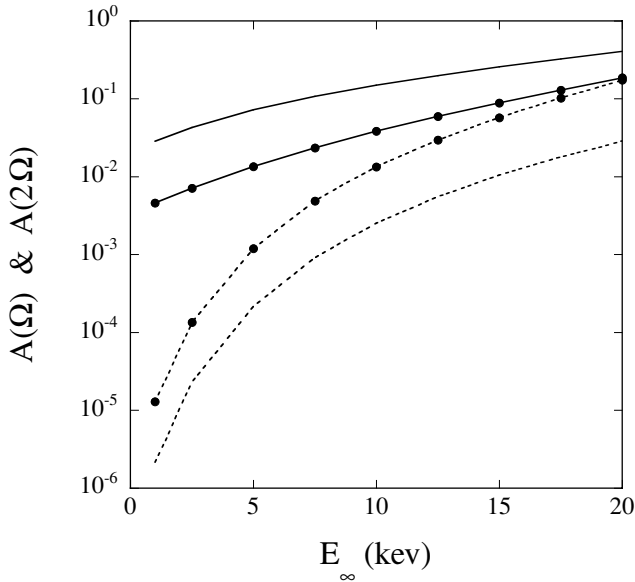


Figure 17. Fourier amplitudes $A(\Omega)$ (solid lines) and $A(2\Omega)$ (dotted lines) as a function of photon energy E_{∞} for the even r mode with $l' = 2$ and $m = 1$ and for the odd r mode with $l' = m = 1$ (filled circles) for $\Omega_{\infty}/2\pi = 400$ Hz, $C_1 = 0.2$, $C_2 = 0$, $\chi = 0$, $i = 60^\circ$, $k_B T_0 = 2.3$ keV, $M = 1.4 M_{\odot}$ and $R = 10$ km.

circles) for $\Omega_{\infty}/2\pi = 400$ Hz, $C_1 = 0.2$, $C_2 = 0$, $\chi = 0$, $i = 60^\circ$, $k_B T_0 = 2.3$ keV, $M = 1.4 M_{\odot}$, and $R = 10$ km. He argued that the increase in the pulsed fraction with increasing photon energy would be useful to identify the mechanism for burst oscillations.

We note that the wave model tends to produce larger-frequency drifts in a burst than are observed (e.g. Heyl 2004). As a possible solution to this difficulty, Piro & Bildsten (2005) proposed that, as the envelope cools toward the tail of a burst, the surface r mode transforms through an avoided crossing into a crustal interface mode, whose frequency remains almost constant during the cooling, perhaps giving a ceiling to the frequency drifts. However, because there occurs at the same time a transformation of the crustal interface mode to the surface r mode through the avoided crossing, in effect the surface r mode could keep its identity during the envelope cooling except in the vicinity of the avoided crossing. That is, it is not obvious from normal mode calculations alone that the r mode will completely transfer its energy into the interface mode. We think that hydrodynamic calculations would be important to further investigate the mode interactions proposed by Piro & Bildsten (2005). Nevertheless, the properties of the surface r modes are likely to be influenced by the existence of the crust, so it is important to further investigate possible mode interactions (see, for example, Lee & Strohmayer 1996; Yoshida & Lee 2001).

Compared with the hotspot model, the wave model generally produces smaller amplitude light variations. This is mainly because the entire surface of the neutron star produces X-ray emission. On the other hand, purely sinusoidal light curves observed for most of the burst oscillators (Muno et al. 2002b) can be explained by assuming the dominance of a single r mode of a given m , and the existence of an appreciable first harmonic component may be attributable to the coexistence of a mode with $2m$, or perhaps a superposition of even and odd modes of different amplitude. As in the case of the hotspot model, the wave model also gives hard leads in most of the parameter space, which may be in conflict with the suggested hard lags seen in some of the burst oscillators, but might be applicable to the hard leads observed from the millisecond X-ray pulsars SAX J1808.4–3658, and IGR J00921+5934 (e.g. Cui et al. 1998; Galloway et al. 2005). The parameters employed in the light-curve calculation include the mass M , the radius R , and the spin frequency Ω of the star, the inclination angle i , the mode indices (m, k, n) , and the oscillation amplitudes C_j . Even if we assume that only the fundamental $n = 0$ r modes with $k = 0$ or $k = 1$ play a role in producing the observed brightness variations and that the frequency that appears in the light curves is the spin frequency of the star, we still have several free parameters that affect the amplitude determination of the light curves. Perhaps the most crucial parameters are the oscillation amplitudes, C_j , themselves, which are difficult to determine within the framework of linear pulsation theory. Further theoretical studies combined with model fitting to the observed properties of burst oscillations will definitely be desired for a better understanding of the burst oscillations and the underlying neutron stars.

REFERENCES

- Arras P., Flanagan E. E., Morsink S. M., Schenk A. K., Teukolsky S. A., Wasserman I., 2003, *ApJ*, 591, 1129
- Bhattacharyya S., Strohmayer T. E., Miller M. C., Markwardt C. B., 2005, *ApJ*, 619, 483
- Braje T. M., Romani R. W., Rauch K. P., 2000, *ApJ*, 531, 447
- Cadeau C., Leahy D. A., Morsink S. M., 2005, *ApJ*, 618, 451
- Chakrabarty D., Morgan E. H., Muno M. P., Galloway D. K., Wijnands R., van der Klis M., Markwardt C. B., 2003, *Nat*, 424, 42

- Chen K., Shaham J., 1989, *ApJ*, 339, 279
- Cui W., Morgan E. H., Titarchuk L. G., 1998, *ApJ*, 504, L27
- Cumming A., Bildsten L., 2000, *ApJ*, 544, 453
- Cumming A., Morsink S. M., Bildsten L., Friedman J. L., Holz D. E., 2002, *ApJ*, 564, 343
- Ford E. C., 1999, *ApJ*, 519, L73
- Frank J., King A., Raine D., 2002, *Accretion Power in Astrophysics*, 3rd edn. Cambridge Univ. Press, Cambridge
- Galloway D. K., Markwardt C. B., Morgan E. H., Chakrabarty D., Strohmayer T. E., 2005, *ApJ*, 622, L45
- Heyl J. S., 2004, *ApJ*, 600, 939
- Heyl J. S., 2005, *MNRAS* (doi:10.1111/j.1365-2966.2005.09183.x)
- Lee U., 2004, *ApJ*, 600, 914
- Lee U., Saio H., 1987, *MNRAS*, 225, 643
- Lee U., Saio H., 1993, *MNRAS*, 261, 415
- Lee U., Strohmayer T. E., 1996, *A&A*, 311, 155
- Lindblom L., Tohline J. E., Vallisneri M., 2002, *Phys. Rev. D.*, 65, 084039
- Longuet-Higgins M. S., 1968, *Phil. Trans. R. Soc.*, 262, 511
- Muno M. P., Chakrabarty D., Galloway D. K., 2002a, *ApJ*, 580, 1048
- Muno M. P., Özel F., Chakrabarty D., 2002b, *ApJ*, 581, 550
- Muno M. P., Özel F., Chakrabarty D., 2003, *ApJ*, 595, 1066
- Nath T. R., Strohmayer T. E., Swank J. H., 2002, *ApJ*, 564, 353
- Page D., 1995, *ApJ*, 442, 273
- Pechenick K. R., Ftaclas C., Cohen J. M., 1983, *ApJ*, 274, 846
- Pedlosky J., 1987, *Geophysical Fluid Dynamics*, 2nd edn. Springer, New York
- Piro A. L., Bildsten L., 2005, *ApJ*, preprint (astro-ph/0502546)
- Poutanen J., Gierliński M., 2003, *MNRAS*, 343, 1301
- Spitkovsky A., Levin Y., Ushomirsky G., 2002, *ApJ*, 566, 1018
- Strohmayer T. E., 1992, *ApJ*, 388, 138
- Strohmayer T. E., Bildsten L., 2004, in Lewin W. H. G., van der Klis M., eds, *Compact Stellar X-Ray Sources*. Cambridge Univ. Press, Cambridge
- Strohmayer T. E., Lee U., 1996, *ApJ*, 467, 773
- Strohmayer T. E., Markwardt C. B., 1999, *ApJ*, 516, L81
- Strohmayer T. E., Zhang W., Swank J. H., Smale A., Titarchuk L., Day C., Lee U., 1996, *ApJ*, 469, L9
- Strohmayer T. E., Jahoda K., Giles B. A., Lee U., 1997, *ApJ*, 486, 355
- Strohmayer T. E., Zhang W., Swank J. H., White N. E., Lapidus I., 1998a, *ApJ*, 498, L135
- Strohmayer T. E., Zhang W., Swank J. H., Lapidus I., 1998b, *ApJ*, 503, L147
- Strohmayer T. E., Markwardt C. B., Swank J. H., in 'T Zand J., 2003, *ApJ*, 596, L67
- Unno W., Osaki Y., Ando H., Saio H., Shibahashi H., 1989, *Non-radial Oscillations of Stars*, 2nd edn. University of Tokyo Press, Tokyo
- van der Kils M., 2004, in Lewin, W. H. G., van der Klis M., eds, *Compact Stellar X-ray Sources*. Cambridge Univ. Press, Cambridge, in press (astro-ph/0410551)
- Weinberg N., Miller M. C., Lamb D. Q., 2001, *ApJ*, 546, 1098
- Yoshida S., Lee U., 2001, *ApJ*, 546, 1121

This paper has been typeset from a $\text{\TeX}/\text{\LaTeX}$ file prepared by the author.